Received: 21 November 2022 | Revised: 9 May 2023 | Accepted: 7 July 2023

DOI: 10.1111/psyp.14396

PSYCHOPHYSIOLOGY SPR WILEY

ORIGINAL ARTICLE

The oscillatory fingerprints of self-prioritization: Novel markers in spectral EEG for self-relevant processing

Céline C. Haciahmet[1] | **Marius Golubickis**[2] | **Sarah Schäfer**[1] | **Christian Frings**[1] | **Bernhard Pastötter**[1]

[1]University of Trier, Trier, Germany
[2]University of Aberdeen, Aberdeen, UK

Correspondence
Bernhard Pastötter, University of Trier, Universitätsring 15, Trier 54286, Germany.
Email: pastoetter@uni-trier.de

Funding information
Deutsche Forschungsgemeinschaft, Grant/Award Number: SCHA 2253/1-1

Abstract

Self-prioritization is a very influential modulator of human information processing. Still, little is known about the time-frequency dynamics of the self-prioritization network. In this EEG study, we used the familiarity-confound free matching task to investigate the spectral dynamics of self-prioritization and their underlying cognitive functions in a drift-diffusion model. Participants ($N = 40$) repeatedly associated arbitrary geometric shapes with either "the self" or "a stranger." Behavioral results demonstrated prominent self-prioritization effects (SPEs) in reaction time and accuracy. Remarkably, EEG cluster analysis also revealed two significant SPEs, one in delta/theta power (2–7 Hz) and one in beta power (19–29 Hz). Drift-diffusion modeling indicated that beta activity was associated with evidence accumulation, whereas delta/theta activity was associated with response selection. The decreased beta suppression of the SPE might indicate more efficient sensorimotor processing of self-associated stimulus–response features, whereas the increased delta/theta SPE might refer to the facilitated retrieval of self-relevant features across a widely distributed associative self-network. These novel oscillatory biomarkers of self-prioritization indicate their function as an associative glue for the self-concept.

KEYWORDS

Drift-diffusion model, matching task, self-prioritization, time-frequency analysis

1 | INTRODUCTION

The fundamental concept of the self is a topic of century-long research (James, 1890), with a widespread interest in the neural basis of the self. The conceptual self can be based on a gradient integration of self-relevant information, including interoceptive, exteroceptive, and mental processing levels of the self (Qin et al., 2020). In particular, the mental processing level addresses representations of non-physical properties such as personality traits or autobiographical memories. This three-level integration process of the self can be depicted by increasing activation of the neural self-network (Qin et al., 2020). The mental processing level of the self is typically deducted from the preferential processing of self-related information in experimental studies. Self-preference is found in multiple

cognitive processes such as attention (for a review, see Sui & Rotshtein, 2019), memory (Dastjerdi et al., 2011; Mu & Han, 2010; Yin et al., 2021), and cognitive control (Golubickis & Macrae, 2021b)—even in 6-month-old infants (Imafuku et al., 2014). The mechanisms behind self-prioritization are versatile: Self-referential information is linked to an elaborated network of domain-general and task-specific self-representations in the brain (Qin et al., 2020; Yankouskaya & Sui, 2022) and thus, might lead to facilitated neural processing and consequently, to a self-bias in behavior. The question of how a self-relevance network in the brain might be organized or communicate with its subregions is unanswered to date.

Preference for self-information modulates a variety of human behaviors. Self-bias has been described previously in terms of the own-name effect in dichotomic listening studies (Moray, 1959), or the own-face effect in visual search paradigms. These self-bias effects reflect a preferential (e.g., faster and more accurate) processing of the own name or face among other names or faces. For instance, participants make fewer errors in judging their own face's orientation than other faces (Keyes & Dlugokencka, 2014; Ma & Han, 2010; Sui & Han, 2007). To avoid familiarity confounds of the own name or face, Sui et al. (2012) introduced a simple paradigm to associate arbitrary geometric shapes with the self or non-self-relevant others. In this paradigm, participants learn associations between shapes and, for instance, the self, a stranger, and a mother label (e.g., circle–me, triangle–stranger, square–mother). In the matching task of the paradigm, participants are instructed to decide whether presented label–shape pairings are matching the originally learned association or whether they are re-paired compared to the learning phase. A self-prioritization effect (SPE) is observed in that self-matching trials require shorter reaction time (RT) and produce fewer errors than other-matching trials. This is typically understood as an indication that random objects can be associated with the self, which will result in prioritized processing of the previously random object (compared to objects that were associated with a stranger, a friend, or the own mother).

The SPE in the matching task is a rather objective indicator for self-processing. It avoids a familiarity confound, which occurred in paradigms using highly familiar and overlearned self-related stimuli, for example, the own name or face. A prioritization of such overlearned stimuli stems from the fact that information processing prioritizes familiar, that is, frequently encountered stimuli. Consequently, the matching of random objects with the self avoids the overestimation of self-prioritization effects. The SPE has been replicated among many studies in different sensory modalities and with different stimuli sets and has been shown to be independent of stimulus arrangement (Golubickis & Macrae, 2021a; Schäfer et al., 2015; Woźniak & Knoblich, 2019).

So far, neural representations of various self-effects have been investigated in specific contexts. Electrophysiological (EEG) studies to date have been investigating self-relevant processing, for example, processing of the own name, the own face, and also the SPE with arbitrarily associated stimuli (Gray et al., 2004; He et al., 2018; Keyes et al., 2010; Knyazev, 2013). These studies mainly report event-related potentials (ERPs) regarding self-processing, that is, the phase-locked and time-locked components of the electrophysiological signal. In general, self-related processing is typically linked to rather early components such as the N2 or N1 in the case of the own-face bias, and rather late components such as the P3 in the case of the own-name bias (e.g., Eichenlaub et al., 2012; Nijhof et al., 2022; Tacikowski et al., 2014). In detail, the own face (compared to other faces) evokes comparatively early increased posterior and fronto-central negativity within 170 ms (N1; Keyes et al., 2010) or 280–340 ms (N2; Sui et al., 2006) after stimulus onset. The P3 is a rather late component in the attention domain, sometimes lasting up to 500 ms after stimulus onset (Knyazev, 2013). In general, the P300 is an evoked response to salient or motivationally relevant stimuli (Knyazev, 2013), for example, for self-relevant possessive pronouns (Zhou et al., 2010) or self-relevant label-face pairings (Woźniak et al., 2018). These ERP findings are often interpreted as indices for attentional advantages of self-related information, although there seem to be boundaries to these explanations (e.g., focal presentation of self-relevant stimuli is necessary to find the SPE; Keyes & Dlugokencka, 2014; Schäfer et al., 2020).

The search for spectral EEG markers of the SPE in the time-frequency domain is of great interest because neural network communication might vary over time scales and frequencies. In general, collaborating brain regions form a transient neural network by structuring temporal windows for neurons to fire simultaneously. This neural communication process is typically dependent on phase dynamics, for instance, coherence patterns in brain oscillations among distributed neural networks (Fries, 2005). Indeed, few studies have investigated spectral EEG signals in self-related research. For example, hand ownership and spatial location of the self in virtual reality can be reflected in alpha band activity (8–13 Hz; Lenggenhager et al., 2011). In a different task, self-referential personality traits were characterized by event-related synchrony in the frontal theta band (4–8 Hz) and central alpha band (Mu & Han, 2010, 2013). Concerning the own-face effect, evoked oscillatory responses to the own face could be found in theta power over frontal midline structures (Miyakoshi et al., 2010), or in suppression of alpha and beta power in response to the own face (Alzueta et al., 2020). Lastly,

autobiographical memory retrieval of self-relevant episodes was associated with changes in gamma band activity (30–180 Hz; Dastjerdi et al., 2011). In sum, a broad variety of frequency bands were reported in these studies, maybe mirroring task-specific and domain-specific aspects of the self rather than a domain-general self-concept. Consequently, to observe the neural signature of the core self-representation, it is important to use a familiarity confound-free paradigm such as the associative matching task (Sui et al., 2012), which relies on randomly assigned objects or shapes instead of highly familiar concepts.

Additionally, computational modeling can be used to figure out the latent cognitive factors mediating the processing advantage of self-prioritization (Falbén et al., 2020). In a hierarchical drift-diffusion model (HDDM), the human system gathers information until one of the binary response thresholds will be reached and either a correct or a wrong response will be initiated. Previous research utilizing cognitive modeling has established that self-relevance during shape–label-matching task modulates evidence sampling speed during stimulus processing (Falbén et al., 2020; Golubickis et al., 2017, 2020; Svensson et al., 2022). This describes the faster and more efficient accumulation of self-relevant information compared to the accumulation of other-relevant information, for example, objects owned by a friend or a stranger (Falbén et al., 2020; Golubickis et al., 2017). This advantage of self-information can be explained by improved attentional processing (Alexopoulos et al., 2012; Sui & Rotshtein, 2019), or improved visual awareness (Macrae et al., 2017). One of the key benefits of integrating computational models of cognition with neural data is that it allows researchers to formulate explicit inferences about the specific task-related cognitive processes associated with EEG signals (Forstmann et al., 2016; Forstmann & Wagenmakers, 2015; Ratcliff et al., 2016). Of particular interest is a recent study by Sui et al. (2023) reporting EEG markers of the SPE in the matching task. Sui et al. (2023) linked the neural time course of self-prioritization with the latent cognitive operations underlying the SPE. In particular, the posterior N1 was related to the rate of information uptake, indicating that self-associated matches profit from faster evidence accumulation (i.e., drift rate, v). In contrast, the rather late centro-parietal P3 was related to the response selection process, indicating that self-associated matches profit from faster response initiation (i.e., boundary separation, a). Interestingly, these results suggest that self-prioritization might have an attentional processing advantage due to a higher salience of self-related stimuli—reflected in the faster encoding of stimuli input in the early posterior N1—but also directly affect sensorimotor operations—reflected in the facilitated response selection in the centro-parietal P3 (Sui et al., 2023).

It is not known, however, how these computational underpinnings map onto spectral EEG signals, which index the (de)synchronization of large neural assemblies in response to an event. By investigating the time-locked and (non)-phase-locked electrophysiological characteristics of self-prioritization, our study sheds light on the neural organization, timing, and communication of the self in the brain. Additionally, drift-diffusion modeling (DDM) was adopted in the present EEG study to explore the link between the condition-level spectral EEG components and the processes of decision-making (Cavanagh et al., 2011; Yau et al., 2021). Thus, the present study expands recent recommendations for brain–behavior research (Bridwell et al., 2018) by (i) examining the time-frequency decomposition of neural time-series signals, and (ii) implementing cognitive modeling to investigate functional connections between the observable SPE and its spectral patterns in the brain. In this way, we explore an exciting new pathway to investigate which oscillatory signatures might be involved in self-related decision-making.

We present the first EEG time-frequency study to examine the oscillatory signature of the SPE, which gives insight into the functional pathways of self-prioritization in neural networks. As such, we investigate self-prioritization (self-match vs. stranger-match conditions) in the associative matching task (Sui et al., 2012) in spectral EEG power from 2 to 30 Hz. We expect a significant difference not only between self-match and stranger-match conditions' (i.e., the SPE) behavioral data (RT, accuracy) but also in the EEG time-frequency (theta, alpha, and beta). Computational modeling will elucidate the latent cognitive features of the spectral SPE, and thus cross-validate our EEG results. Based on previous research (Sui et al., 2023), we expected self-prioritization to facilitate the evidence accumulation process, as well as the response selection during decision-making.

2 | METHODS

2.1 | Participants

Forty students from the University of Trier, Germany, were included in the study (32 women, 3 left-handed, mean age = 23.65 years, SD = 3.13 years). Three additional participants were tested but eliminated from the analysis due to below-chance accuracy in the matching task (Acc < .48). The effect sizes for the SPE were large in previous studies ($\eta^2 = 0.67$ in Sui et al., 2012). Given $N = 40$, $\alpha = .05$, a power of $1 - \beta = .90$, and $r = .30$ among repeated measures, a medium-sized or larger effect of $f \geq .25$ could be detected in this study (G*Power 3.1.3, Faul et al., 2007). All participants reported normal or corrected-to-normal

vision and no participant reported any history of neurological disease. All participants gave written informed consent before the examination and received course credit or monetary compensation (15€) for participation. The study was conducted following the Declaration of Helsinki and approved by the local ethics review committee at the University Trier.

2.2 | Design

The associative matching task was adapted from Sui et al. (2012), in which participants learned the mapping of geometric shapes (circle and triangular), to the self, or a stranger, for example, "I am a circle. A stranger is a triangle." After the learning phase, participants indicated whether the briefly presented stimulus–label combinations matched the association rules they had been learning previously. Thus, the experiment consisted of a 2 (stimuli pairings: *self-associated* vs. *stranger-associated*) × 2 (condition: *match* vs. *non-match*) within-participant design.

Following the associative matching task, a second task was conducted to examine the modulation of cognitive control parameters in the EEG by self-prioritization (see Golubickis & Macrae, 2021b, for a similar study rationale with a flanking shape classification task). As the flanker results are not of concern for the present hypotheses, please refer to the Appendix S1 for the description and results of the flanking shape classification task.

2.3 | Stimulus materials and procedure

The matching task had four possible trial types, consisting of two labels ("Ich" in German translates to *me*, and "Fremder" in German translates to a *stranger*) and two shapes (circle and triangle). The to-be-learned shape–label pairings were presented to each participant for 60 s before the experimental phase of the task started. In this experimental phase, participants were instructed to respond via key press on a response box as quickly and accurately as possible whether a presented shape–label pairing matches or non-matches the association learned earlier (see Figure 1b for a single trial course from pupil fixation until response onset). Order of shape–label associations and key–response mapping were randomized and counterbalanced across all participants. The task consisted of 240 trials in sum distributed across 4 blocks (i.e., 120 matching trials and 120 non-matching trials with 60 self-related and 60 stranger-related trials each). After each block, participants took a self-paced short break, during which they were reminded of the correct key–response mapping.

Every trial began with a white fixation cross, which was shown in the center of a computer screen (Eizo S1911, 19 inches, 1280 × 1024) for an interval of a minimum of 1.5 s and a maximum until the eye tracker fixated the pupil. The eye tracker (Eyegaze System, LC Technologies) was calibrated for each subject to control for eye movements and blinks during EEG recording. The eye tracker identified a correct pupil fixation within a radius of 1.77 cm (or 60 pixel) around the fixation cross. After the presentation of the fixation cross, the shape–label pairing was shown for 100 ms in the middle of the screen: The geometric shape was shown above and the label was shown below the center of the screen. The top/bottom presentation of shape and label presentations was fixed across all trials to avoid eye movements during the EEG recording. All labels were written in white on black background, whereas the geometric shapes were gray on black background. Shapes were approximately 2.2 cm × 2.2 cm in size at a viewing distance of 60 cm. The letters were written in Courier New font with 0.5 cm in size and 0.5 cm distance to the geometric shape. Participants were told to maintain their fixation on the center of the screen and not move their eyes. After 100 ms, the shape–label pairing disappeared and participants saw a black screen until they responded with a keypress by their left or right index finger (or until 1.5 s have passed). No feedback was provided in the experimental session. After the key was pressed on the Chronos response box (Chronos™, Science Plus Group) or after a maximum of 1.5 s, the next trial started with the presentation of the fixation cross. To familiarize participants with the procedure, they were given one block of 24 practice trials with feedback (right, wrong, and too slow) shown for 0.5 s before the experiment. The experimental session of the matching task took about 15 min. Presentation and recording of behavioral responses were done with E-Prime software (v2.0, Psychology Software Tools).

2.4 | Analysis of behavioral data

Both mean RT and error rates were analyzed in JASP (version 0.16.3; JASP Team, 2022). For RT analysis, only trials were included for which responses on both the current trial (n) and the previous trial (n–1) were correct. Moreover, only responses greater than 200 ms and smaller than 1 s were included in the analysis following Ulrich et al. (2015). In total, less than 0.7% of trials were excluded from the HDDM analysis. Behavioral data for the matching task were analyzed with repeated-measures ANOVAs with the factor stimuli association (self vs. stranger), condition (match vs. non-match), and the dependent variables RTs and accuracy rate. All statistical tests were analyzed two-sided. Greenhouse–Geisser corrections

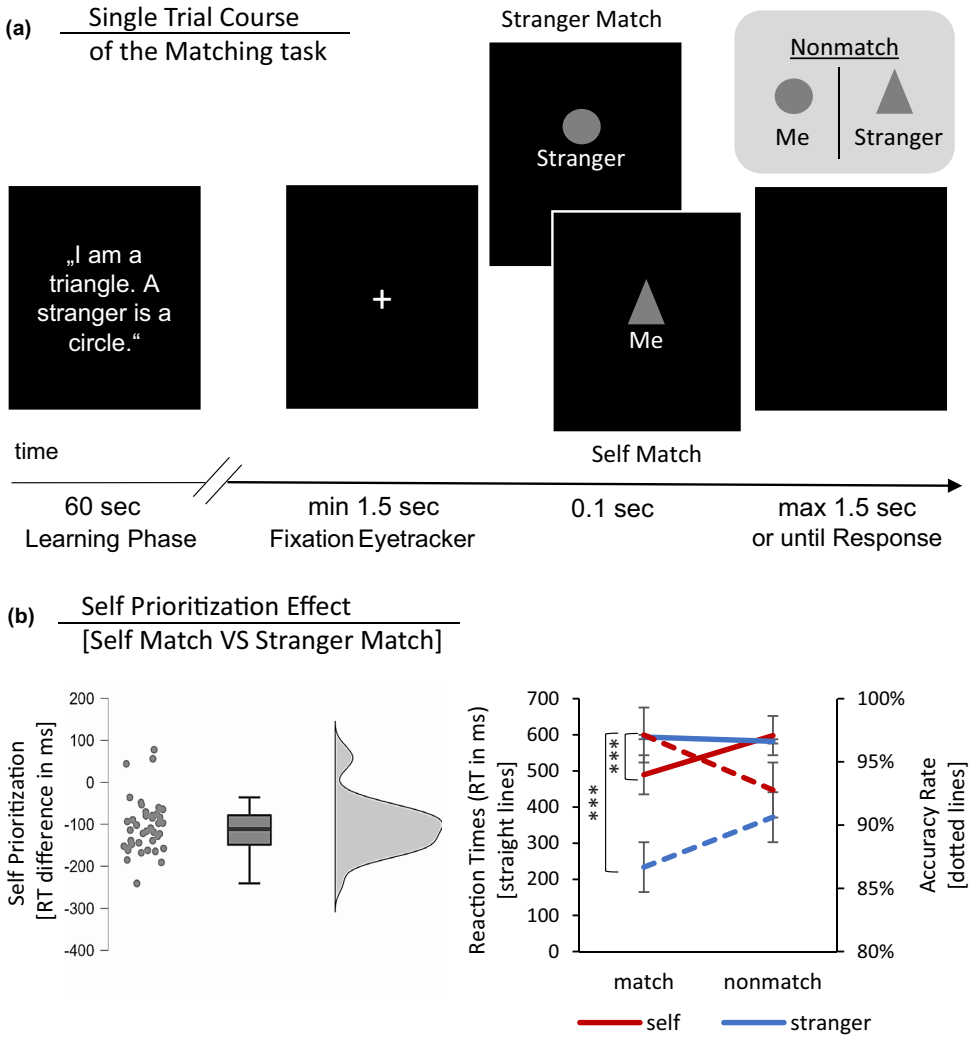

FIGURE 1 Overview and results for the matching task. (a) Overview of a single trial time course in the matching task. (b) Raincloud plot of the self-prioritization effect (*self-match* minus *stranger-match*) in RT. SE according to Cousineau and O'Brien (2014) in the line chart ("***" indicates $p<.001$).

were applied where appropriate. Significant interaction effects were further examined with simple contrast comparisons. Significant results will be reported with appropriate effect sizes (η_p^2), whereas non-significant results will be specified by Bayes factor BF_{01}, which indexes the relative support in the observed data for the *H*0 versus the *H*1, assuming a uniform prior distribution on the correlation parameter Pearson's ρ (Hoijtink et al., 2019).

2.5 | Recording of EEG data

Electrophysiological data were recorded from 65 Ag/AgCl electrodes, which were positioned according to the 10–10 electrode system with reference to CPz (EC80, Montage No. 1, Easycap). The ground was placed at location FPz. The electrooculogram (EOG) was recorded from four bipolar channels, positioned on the inferior and superior regions of the left eye and the outer canthi of both eyes, to monitor the vertical and horizontal EOG. Electrode-skin impedance was kept below 5 kΩ for all electrodes. Signals were digitalized with a sampling rate of 500 Hz and amplified between 0.016 and 250 Hz (BrainAmp, BrainVision Recorder, v1.20, BrainProducts).

2.6 | Pre-processing of EEG data

EEG recordings were re-referenced offline against average reference and EOG was corrected by using calibration data and generating individual EOG artifact coefficients, as implemented in BESA Research (v7.1, BESA Software). The remaining artifacts were marked by visual inspection. EEG data were segmented into epochs ranging from −1.3 to 1.3 s around the onset of stimuli and from −1.9 to 0.7 s around the onset of responses. Segments containing

artifacts and segments with response errors either on the current (n) or on the previous trial (n−1) were discarded from further analysis. For response-locked analysis, on average, 38 self-match trials ($SE = 0.57$), 37 self-non-match trials ($SE = 0.62$), 35 stranger-match trials ($SE = 0.80$), and 35 stranger-non-match trials ($SE = 0.69$) went into cluster analysis after artifact correction. For stimulus-locked analysis, on average, 38 self-match trials ($SE = 0.58$), 37 self-non-match trials ($SE = 0.62$), 35 stranger-match trials ($SE = 0.80$), and 35 stranger-non-match trials ($SE = 0.69$) went into cluster analysis after artifact correction.

2.7 | Spectral EEG analysis

The EEG data were transformed into the time-frequency domain using a demodulation algorithm, which is implemented in BESA Research (v7.1). The algorithm consists of a multiplication of the time domain signal with a periodic exponential function, having a frequency equal to the frequency under analysis, and subsequent low-pass filtering. The low-pass filter is a finite impulse response filter of Gaussian shape in the time domain, which is related to the envelope of the moving window in wavelet analysis. The data were filtered in a frequency range from 2 to 30 Hz. The time resolution was set to 78.8 ms (full power width at half maximum; FWHM), and the frequency resolution was set to 1.42 Hz (FWHM). Time-frequency data were exported in bins of 50 ms and 1 Hz. Both stimulus- and response-locked power changes were calculated, time locked to stimulus or response onset, respectively. Stimulus- and response-locked changes in power were determined by calculating the temporal-spectral evolution, that is, power changes for all time-frequency points with power increases or decreases at time point t and frequency f related to mean power at frequency f over a preceding baseline interval (Pfurtscheller & Aranibar, 1977). Stimulus-locked power changes were determined with a pre-stimulus baseline interval that was set from −800 to −300 ms time locked to stimulus onset, whereas response-locked power changes were determined with a baseline interval that was set from −1400 to −900 ms time locked to response onset for the matching task.

2.8 | Cluster analysis of spectral EEG

Time-frequency characteristics of stimulus-locked effects after stimulus onset (0 to 400 ms) in a frequency range from 2 to 30 Hz were examined with permutation-based cluster analysis as implemented in BESA Statistics (v2.1, BESA Software). A cluster analysis was computed for the SPE in match trials, that is, for power difference between self-match and stranger-match conditions. A non-spatial cluster analysis was calculated first and a spatial analysis was calculated second. In the non-spatial cluster analysis, time-frequency spectrograms of power changes were averaged across the 65 electrodes and contrasted between conditions. For the contrast between the SPE conditions, two-tailed t-tests were calculated for all time-frequency points (9 [50 ms time bins] × 29 [1 Hz frequency bins] × 65 [electrodes]). The sum of t-values of adjacent time-frequency points that fell below a p-value of .05 in the t-test was calculated as a test statistic. Random permutation analysis was calculated based on 1000 randomization runs. In each randomization run, time-frequency data of the two conditions were interchanged randomly for each participant, and t-tests were calculated for each time-frequency point. At the end of each run, t-values of adjacent time-frequency points that fell below a p-value of .05 were summed and the cluster with the highest sum of t-values was kept. By these means, a null distribution of cluster sums was created from the 1000 permutation runs, and the critical p_{crit} value for an empirically derived time-frequency cluster was estimated. Next, empirical clusters with a $p$crit value below .01 went into spatial analysis. For each cluster, power changes were averaged across data points of the cluster's maximum time range and maximum frequency range, separately for each electrode. These data were contrasted between conditions. Two-tailed t-tests were calculated for all electrodes. Spatial topographies were identified by considering those electrodes that fell below a p-value of .01 in the t test. Thus, both clustered and scattered effects of conditions were considered in the spatial analysis. Lastly, (two-sided) paired-samples t tests were computed for each significant cluster for the SPE in match trials (self-match vs. stranger-match) in JASP (version 0.16.3; JASP Team, 2022), which were further specified by Cohen's d as appropriate effect size.

2.9 | Drift-diffusion modeling

The DDM uses both response reaction time and accuracy to estimate the latent cognitive processes associated with task performance and how they unfold over time (Ratcliff et al., 2016). During binary decision-making (e.g., is a shape–label pairing matching or non-matching), evidence is continuously gathered from a stimulus until one or other response threshold has been reached. The benefit of sequential sampling models, such as the DDM, lies in the ability to identify the stimulus- and/or response-related processes that underpin task performance (Ratcliff et al., 2016; Voss et al., 2013; White & Poldrack, 2014). In this respect, the DDM comprises four parameters that describe the dynamics of decision-making. First, drift rate (v)

estimates the quality and speed of evidence sampling (i.e., larger v = faster information uptake). This component represents noisy information accumulation during decision-making, and thus is treated as a measure of stimulus processing efficiency. The second parameter is boundary separation (a). It quantifies the space (i.e., distance) between the two response thresholds, and thus refers to the amount of information required before a judgment is made. Large values of a represent a conservative and cautious decision-making style, whereas small values signal a more liberal, less careful approach. Next, between the two response boundaries, the starting point (z) specifies the position at which the noisy information sampling process begins. In situations in which z is not centered between the boundaries, the starting point represents a response bias in favor of the nearer boundary (i.e., variation in the evidential requirements of response selection). Finally, all processes that do not contribute to decision-making (e.g., stimulus encoding and response execution) are described by the non-decision time parameter (t_0).

To elucidate the origins of self-prioritization, a hierarchical drift-diffusion model (HDDM) analysis was conducted on the data (Vandekerckhove et al., 2011). HDDM is an open-source Python toolbox for the hierarchical Bayesian computation of DDM decisional components (Wiecki et al., 2013). The HDDM treats model parameters for individual participants as random samples constrained by group-level distributions (Vandekerckhove et al., 2011). Following previous research that explored computational underpinnings during shape–label matching task (Golubickis et al., 2017, 2020; Svensson et al., 2022), the models were response coded (i.e., upper threshold = match response, lower threshold = non-match response). For each estimated model, 3000 Markov Chain Monte Carlo (MCMC) samples (300 burn-in) were simulated. The deviance information criterion (DIC) was adopted as a measure of fit for the model comparisons (Spiegelhalter et al., 1998), where lower DIC values indicate greater fit as they favor models with the least number of parameters and highest likelihood.

3 | RESULTS

3.1 | Self-prioritization is found in RTs and error rates

Mean RTs and accuracy rates for the SPE are shown in Figure 1. A repeated-measures ANOVA with RTs and the factors stimulus association (self-associated vs. stranger-associated) and matching condition (match vs. non-match) revealed significant main effects of stimuli association, $F(1, 39) = 65.28$, $p < .001$, $\eta_p^2 = .626$, and matching condition, $F(1, 39) = 83.84$, $p < .001$, $\eta_p^2 = .683$, as well as a significant interaction between both factors, $F(1, 39) = 112.31$, $p < .001$, $\eta_p^2 = .742$. Most importantly, a simple contrast in the matching condition showed a significant SPE, $t(77.90) = 13.24$, $p < .001$, indicating significantly faster responses in self-relevant matching trials ($M = 489$ ms, $SE = 13$ ms) than in stranger-relevant matching trials ($M = 594$ ms, $SE = 13$ ms). For the accuracy rates, a repeated-measures ANOVA with the factors of stimulus association (self-associated vs. stranger-associated) and matching condition (match vs. non-match) did not reveal a significant main effect of matching condition, $F(1, 39) = 0.11$, $p = .742$, $BF_{01} = 5.80$, but a significant interaction between stimuli association and matching condition, $F(1, 39) = 19.31$, $p < .001$, $\eta_p^2 = .331$, as well as a significant main effect of stimulus association, $F(1, 39) = 50.51$, $p < .001$, $\eta_p^2 = .564$. The significant interaction was qualified by a significant simple contrast between the self-match and the stranger-match condition, $t(77.69) = -8.07$, $p < .001$, indicating the SPE also in accuracy parameters. Participants responded correctly in 97.1% ($SE = 0.6\%$) of the self-match trials compared to correct responses in 86.7% ($SE = 1.3\%$) of the stranger-match trials.[1]

3.2 | Beta and delta/theta power increases represent the spectral signature of the SPE

The cluster analysis was computed for the SPE in self-match versus Stranger-match trials (see Figure 2). First, non-spatial cluster analysis, time locked to stimulus onset, revealed two significant clusters for the SPE in match trials in desynchronized beta power and synchronized delta/theta power (see Figure 2a). In a further step, spatial cluster analyses were computed to specify the scalp topography of the spectral effects (see Figure 2b,c for the SPE in match trials).

A significant increase in delta/theta power (2–7 Hz; see Figure 2b) was observed for the SPE in a time window from 200 to 400 ms post-stimulus onset, $p < .001$. The peak latency of the delta/theta cluster was around 400 ms following stimulus onset. The cluster showed a scattered, mostly right hemispheric topography around peak electrodes POz and FT7 (electrodes F1, Fz, F4, FC6, C2, C4, T8, CP1, CP2, P3, P1, Pz, P2, POz, and FT7, FC5, T7, C5, TP9;

[1]Behavioral differences for the shape (triangle and circle) were tested by conducting paired samples t-tests between all trials with each shape. Both of these tests were not significant, $t(39) = 0.43$, $p = .672$, $BF_{01} = 5.38$ in RT and $t(39) = -0.95$, $p = .349$, $BF_{01} = 3.86$ for accuracy rates, indicating that no significant shape preference was observed on the group level.

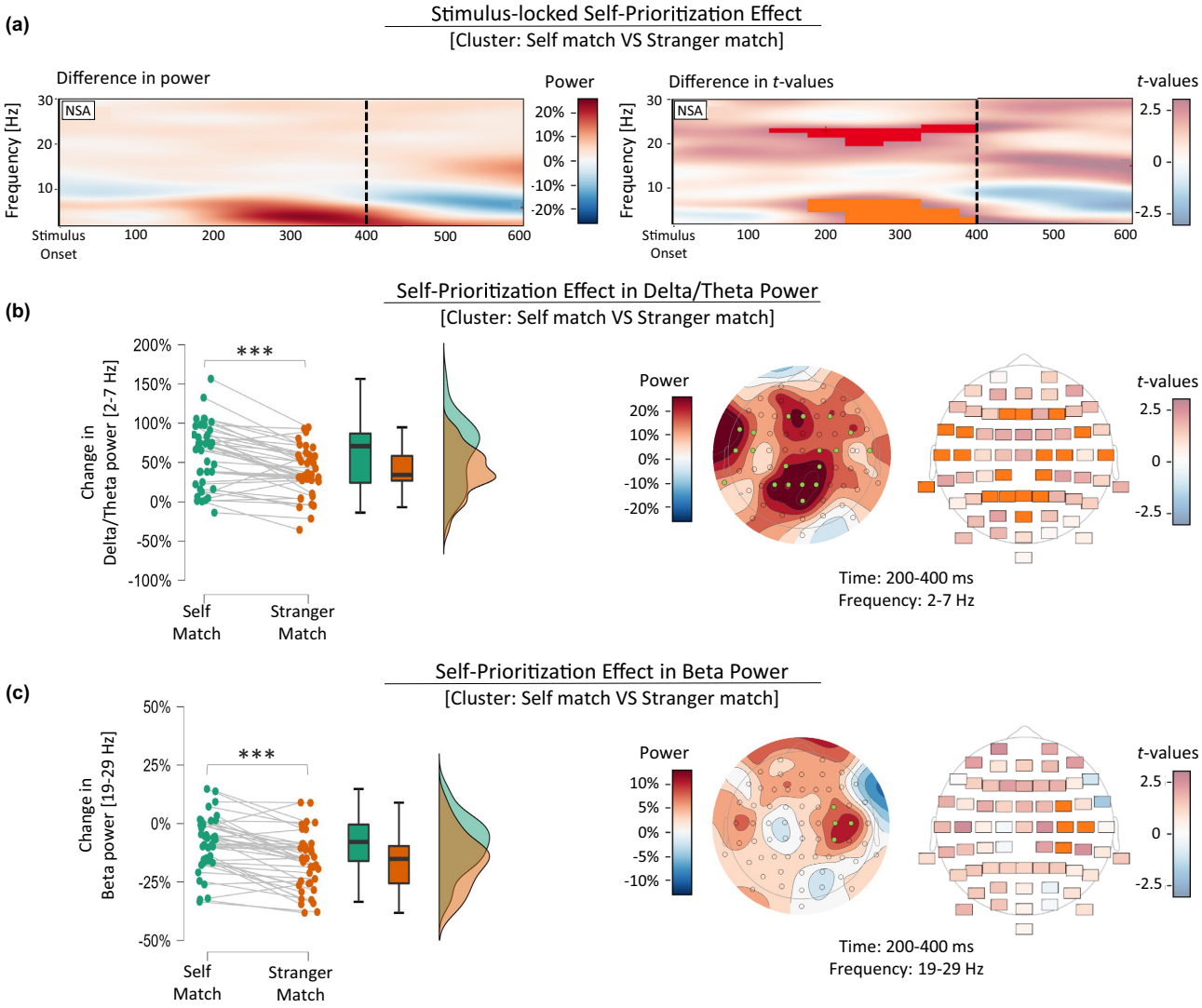

FIGURE 2 Spectral EEG results of the stimulus-locked self-prioritization effect in match trials (SPE; power difference between self-match and stranger-match). (a) Two significant clusters emerged: a relative power increase for the SPE in delta/theta power (b) and beta power (c), both clusters emerging from 200 to 400 ms after stimulus onset. The dotted lines at 400 ms after stimulus onset show the end of the time window for the cluster analysis. The raincloud plots on the left show the individual differences between self-match and stranger-match trials for each participant. Significant cluster electrodes in the topographical plots on the right are depicted in green color (power plots) and orange color (*t*-value plots) ("***" indicates $p<.001$).

see Figure 2b). Self-match trials showed overall higher delta/theta power increase ($M=60.7\%$, $SE=6.3\%$) than stranger-match trials ($M=38.6\%$, $SE=4.8\%$), $t(39)=5.46$, $p<.001$, Cohen's d = 0.864.

Second, a significant decrease in beta power (19–29 Hz; see Figure 2c) was observed for the SPE in a time window from 200 to 400 ms post-stimulus onset, $p<.001$. Peak latency was around 250 ms after stimulus onset. The beta power cluster showed a mostly right hemispheric topography around peak electrode C4 (electrodes FC4, C4, CP4, C6; see Figure 2c). Self-match trials showed overall a lower beta power decrease ($M=-8.8\%$, $SE=1.9\%$) than stranger-match trials ($M=-16.4\%$, $SE=1.9\%$), $t(39)=6.00$, $p<.001$, Cohen's d = 0.948. Further analyses regarding the event-related potentials (ERPs) for the SPE are reported in the Appendix S1.

3.3 | The EEG time-frequency effects for the SPE are good fitting parameters in the drift-diffusion model of the behavioral SPE

Several models were estimated for comparison to identify condition-level correlations between brain measures (i.e., the SPEs in EEG time-frequency signals, see Figure 2) and DDM parameters using HDDMRegression function. Previously, a model that allowed the drift rate (v) to vary as a

function of stimuli association and experimental condition with a single estimate of the starting point (z), boundary separation (a), and non-decision time (t_0) has been found to be best fitting in shape–label matching tasks (i.e., default model, Golubickis et al., 2017; Golubickis et al., 2020; Svensson et al., 2022). Therefore, all performed models included this parameter setup with the inter-trial variability for drift rate (sv), non-decision time (st), and starting point (sz) and, importantly, allowed condition-level variation of neural activity (i.e., the SPE in beta power, and the SPE in delta/theta power) to modulate decisional parameters. First, we compared two models that allowed drift rate (v) to vary parametrically only with the SPE in beta power (DIC = −3802) or only with the SPE in delta/theta power (DIC = −3793). This revealed that the beta SPE is more strongly associated with the speed of information uptake parameter. Second, a model that varied boundary separation (a) as a function of the delta/theta SPE improved model fit (DIC = −3842) compared to only the beta SPE (DIC = −3706). This suggested that the delta/theta SPE (vs. the beta SPE) is effectively more related to response caution. Finally, informed by prior comparisons, a model that varied parametrically beta SPE onto v and delta/theta SPE onto a was estimated. This parameterization was best fitting (DIC = −3855), even compared to a more complex model that regressed drift rate and boundary separation onto both beta SPE and delta/theta SPE (DIC = −3828).

Replicating prior research (Golubickis et al., 2017, 2020; Svensson et al., 2022), analysis of the posterior distributions revealed that in matching trials there was extremely strong evidence that information uptake (i.e., drift rate) was faster for self-relevant compared to stranger-relevant stimuli ($p_{\text{Bayes}}[\text{self} > \text{stranger}] < .001$, $BF > 1000$), see Figure 3a. In non-matching trials, there was little evidence for a difference between self and stranger-associated items ($p_{\text{Bayes}}[\text{self} > \text{stranger}] = .343$, $BF = 2$), see Figure 3b. In addition, comparing the starting point value (z) with no bias ($z = .50$) yielded extremely strong evidence of a response bias in favor of matching (vs. non-matching) judgments ($p_{\text{Bayes}}[\text{bias} > 0.50] < .001$, $BF > 1000$). For the condition-level EEG regressors, there was extremely strong evidence for an increase in the rate of information uptake as the beta

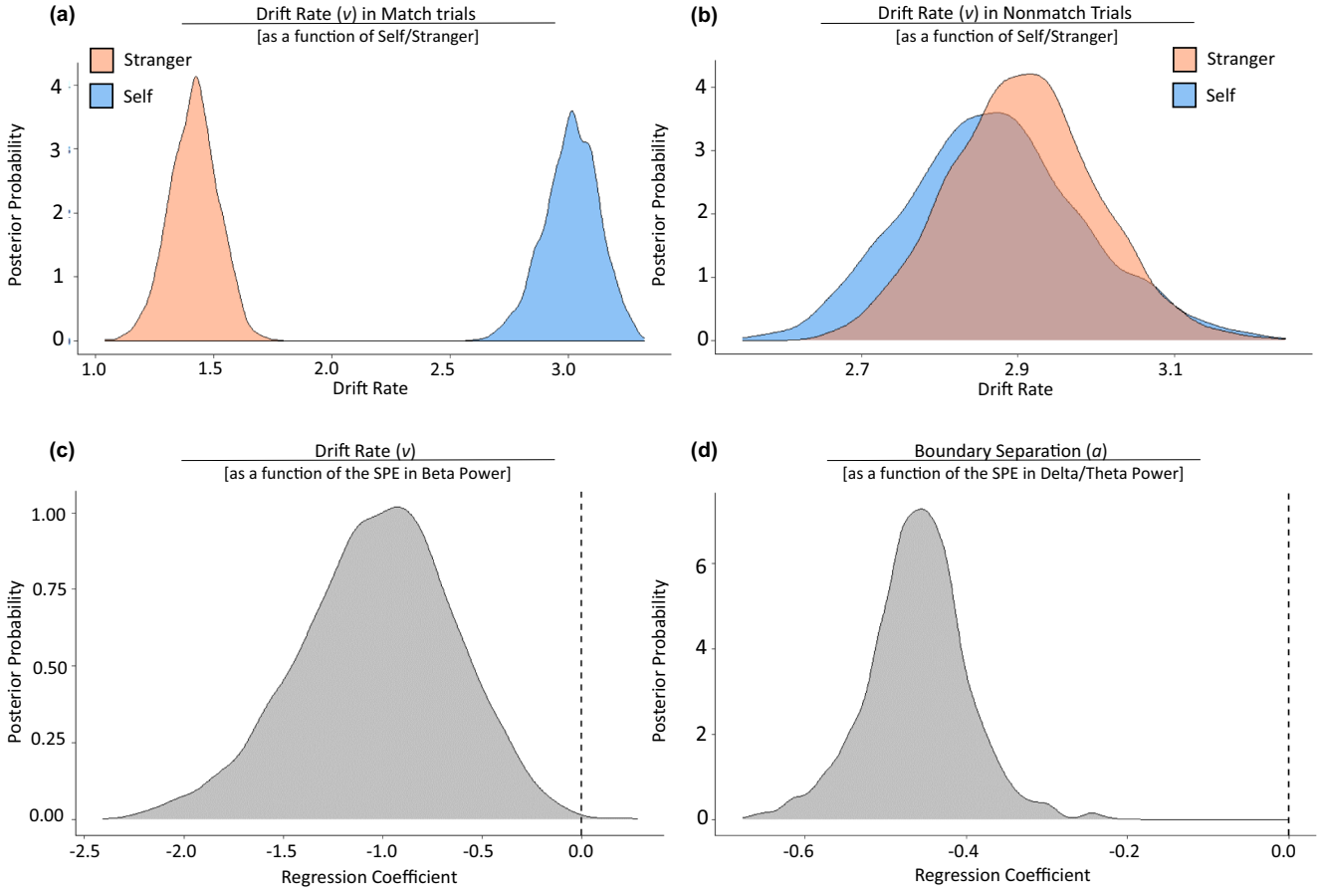

FIGURE 3 Drift-diffusion modeling results for the SPE (difference between self-match and stranger-match conditions). Mean posterior parameter distributions of drift rate (v) as a function of stimuli association and matching condition. The drift rates for self and stranger-associated stimuli are depicted separately for the match condition (a) and for the non-match condition (b). Mean posterior regression coefficient distributions of the SPE in beta power on drift rate (v) (c) and the SPE in delta/theta power on boundary separation (a) (d).

SPE decreased (p_{Bayes}[drift rate ~ beta] = .002, BF = 499), and extremely strong evidence for a decrease in boundary separation as delta/theta SPE amplified (p_{Bayes}[boundary separation ~ delta/theta] < .001, BF > 1000), as can be seen in Figure 4.

4 | DISCUSSION

This study demonstrates self-prioritization effects in the time-frequency domain, namely an increase in delta/theta power (2–7 Hz) and a decrease in beta power (19–29 Hz) for self-associated processing compared to stranger-associated processing. Even without any influence of familiarity, a large SPE occurred (Cohen's d = 1.62 for RT, and Cohen's d = 1.10 for accuracy rate) that was associated with several EEG frequencies.

Within 400 ms after stimulus onset, there were two effects, one in desynchronized beta power (19–29 Hz) and one in synchronized delta/theta power (2–7 Hz) for the self-prioritization effect. The beta SPE started 200 ms after stimulus onset and continued until presumable response onset, hinting at a continuous neural process over the time course. Computational modeling further extends this picture by suggesting that the best model fit with the drift rate (the parameter for gradual evidence accumulation) is represented in the beta power SPE. Specifically, a negative regression coefficient between the behavioral SPE and the beta SPE shows that self-matches induce faster and more efficient encoding of self-relevant information. The event-related decrease in beta power is stronger in stranger-match trials than in self-match trials. In other terms, the human brain gathers more self-relevant input, that is, greater drift rate for self-match trials, while investing less cognitive resources, that is, a smaller decrease in beta power for self-match trials. The right hemispheric topography of the beta SPE raises another important perspective: The beta SPE might be located over or close to the right central sulcus, suggesting the involvement of sensorimotor areas in the right hemisphere. This is particularly interesting as beta power decreases over sensorimotor regions are a typical oscillatory pattern for contralateral response preparation (Gongora et al., 2016; Liebrand et al., 2018). In visuomotor tasks, decision-making requires the coordination of the visual cortex and motor cortex (e.g., supplementary motor area and primary motor cortex), which corresponds to event-related desynchronization in the beta band (Erla et al., 2012; Hosaka et al., 2016). In the present context, beta oscillations might function as a sensorimotor integration process selecting highly salient sensory information, that is, self-relevant objects, to map it onto action plans (Siegel et al., 2011).

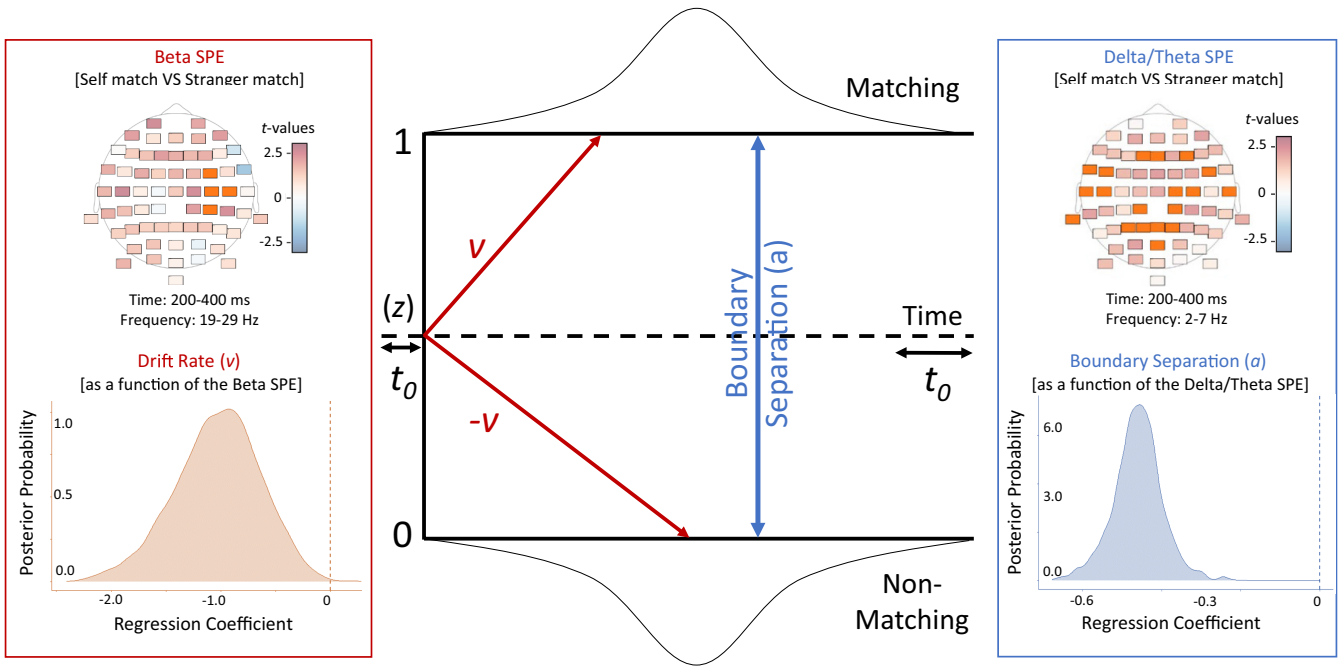

FIGURE 4 Schematic version of the diffusion model results (adapted from Voss et al., 2013, p. 4) for the self-prioritization effect (SPE; self-match vs. stranger-match). An information gathering process begins at starting point z and continues with a mean slope v until it reaches an upper (1) or lower (0) threshold. The drift rate v showed a negative posterior regression coefficient with the beta SPE, whereas the boundary separation a showed a negative relation with the delta/theta SPE. Non-decision processes (t_0) reflect how much time elapses before/after the decision process. Outside the threshold boundaries, the response distributions for matching and non-matching conditions are shown.

Previously, self-relevance has been denoted as an associative glue (Schäfer et al., 2020; Sui & Humphreys, 2015), implying that self-relevance helps to combine particular stimuli with each other. In detail, participants are instructed to learn that geometric shapes are self-relevant, which fastens the integration of those features into an associative "network of importance" (Schäfer et al., 2020). The rather fast and stable process of binding things together highlights similarities with basic binding and integration processes of stimulus features and action features in action-control research (for the general processes of feature integration and binding, see, e.g., the Binding and Retrieval in Action Control [BRAC] framework; Frings et al., 2020; Kiesel et al., 2023; Verguts & Notebaert, 2009). In this context, the self can be represented as jointly bound features (Hommel, 2019) that are weighted by their relevance for the self (Memelink & Hommel, 2013). Following the basic mechanisms of feature integration and retrieval (Frings et al., 2020), the encoding and retrieval of self-relevant features in self-match trials can be assumed to be stronger as compared to stranger trials. This explains why self-relevant shape–label pairings receive enhanced processing while simultaneously co-activating the correct response feature. This co-activation is even stronger in self-relevant trials than in stranger-relevant trials. Hence, in self-relevant matching trials, the processing of a self-relevant stimulus retrieves the related response features even stronger than the processing of a stranger-relevant stimulus does. This sensorimotor processing advantage of the SPE might then be reflected in less pronounced beta power suppression. Beta band activity (BBA) has recently been linked to action control and more precisely to the BRAC framework (Beste et al., 2023; Pastötter et al., 2021). In a nutshell, BBA might reflect the maintenance or transition from active to latent memory of the trial's event file. The strength of BBA may indicate the time window, in which this event file can potentially be re-activated. For self-relevant features, BBA change was increased compared to non-self-relevant features, suggesting prioritized encoding and re-activation of self-relevant material—or more generally better dynamic management of memory traces pertaining to self-associated features. Taken together, this study not only replicates the improved evidence accumulation of self-relevant stimuli (Golubickis & Macrae, 2021b; Svensson et al., 2022) but also reveals further evidence that the encoding of self-associated feature bindings helps to inform more efficient action selection and execution—as indicated by the beta power decrease in self-prioritization.

Additionally, we found evidence for the SPE being represented in the delta/theta frequency (2–7 Hz) range. Increased delta/beta power can be observed in self-match compared to stranger match trials, starting 200 ms after stimulus onset until response execution. There is already first evidence for a link between theta oscillations and preference for self-relevant information: For instance, theta-band-specific synchronization for self-relevant adjectives was observed over frontal regions, which correlated positively with the self-preference effect during memory retrieval (Mu & Han, 2010). Regarding the functional significance of the delta/theta SPE, drift-diffusion modeling suggests that delta/theta activity might correspond with facilitated action selection (see also Herz et al., 2016; Nayak et al., 2019). This decisional bias describes a faster reaching of the response threshold in self-match trials compared to stranger-match trials, thus a more impulsive reaction to self-relevant input. Interestingly, the accuracy for self-match trials is overall higher than for stranger-match trials, arguing against a speed–accuracy trade-off (Pastötter et al., 2012). Alternatively, our result pattern might be an indication of boundary separation reflecting response caution rather than response selection (Lee et al., 2023). This means, faster evidence gathering for self-matching trials leads to more confidence in making a decision, hence a more pronounced negative boundary separation parameter.

In general, slow oscillations in the delta- and theta-frequency range are an ideal communication medium within largely distributed cortical and subcortical structures (Başar et al., 2000; Herweg et al., 2020), for instance, during episodic memory formation (Axmacher et al., 2006; Battaglia et al., 2011). Large neural assemblies of similar cells synchronize their rhythmicity pattern across the brain in the theta-frequency band, for example, to encode or retrieve episodic information. The hippocampal–cortical binding of memory episodes has been repeatedly linked to theta synchronization (Axmacher et al., 2006; Battaglia et al., 2011; Jacobs et al., 2006; Karakaş, 2020). Based on the previously described "network of importance" (Frings & Wentura, 2014; Schäfer et al., 2020), the retrieval process of multiple contextual features such as the triangle, the circle, the letters, and the color might be reflected in the delta/theta frequency. As the "match" pairings correspond best to the initial learning phase, memory retrieval of "old," easily accessible information might be reflected in synchronized delta/theta activity across the scalp. Note that this applies to self-match as well as other-match pairings. The SPE has to be contributed by an additional benefit for self-matches in the human brain (Morel et al., 2014; Sui & Humphreys, 2015): Self-relevance might have served as a weighting mechanism during feature encoding (Memelink & Hommel, 2013), prioritizing self-relevant over other task-relevant context features in the processing stream. As a consequence, the retrieval of self-relevant stimuli in match trials co-activates the jointly bound correct response, which

corresponds to the decreased response threshold for the delta/theta SPE in the present study. In sum, we propose that the retrieval of self-relevant (context) features in the associative self-network might be realized via synchronization in the low-frequency spectrum (2–7 Hz), which in turn modulates the decisional process toward faster, but yet more accurate responses.

This study has several strengths, which confirm the validity and reliability of the proposed oscillatory markers for the SPE. First, we followed best practice guidelines in brain–behavior research, combining cognitive modeling with time-frequency approaches (Bridwell et al., 2018). Second, the drift-diffusion modeling revealed very strong evidence ($BF > 1000$) for the regression analyses between the behavioral SPE and the neural SPE clusters. Third, we report similar SPE findings compared to Sui et al. (2023), see also the ERP analyses in the Appendix S1. Specifically, Sui et al. (2023) presented two ERP components distinctively linked to evidence accumulation (associated with the posterior N1) and response selection (associated with the centro-parietal P3) for self-associated matches compared to other-associated matches. We also found two EEG time-frequency clusters indicating more efficient stimulus encoding and response initiation. Although ERP components and time-frequency markers do not always share the same underlying neural origin or cognitive mechanism, it is interesting to see that the posterior P300 in the present study correlated positively with the delta/theta SPE cluster (uncorrected correlation, which lost statistical significance after Bonferroni correction). The similarities of both studies (Sui et al., 2023) might contribute to the reliability of the present results on one side, while also encouraging future EEG studies to implement cognitive modeling approaches on the other side.

Concerning the scattered topographical plot of the delta/theta SPE over parietal, temporal, mid-central, and mid-frontal electrode sites, various brain regions likely contribute to the improved decisional process of self-prioritization. It is common to observe a spatially scattered time-frequency cluster in theta power during memory retrieval (Herweg et al., 2020), possibly related to distinct processing of recollection and memory interference across time and space (Pastötter & Bäuml, 2014). However, other higher-order structures might also be involved in the delta/theta SPE, such as the vmPFC (Yankouskaya et al., 2017; Yankouskaya & Sui, 2021; Yin et al., 2021), or cortical midline structures, such as the pregenual ACC (Hu et al., 2016; Murray et al., 2015), that are commonly associated with the core of self-representations (Moran et al., 2009; Murray et al., 2015; Sui & Humphreys, 2015). As the EEG is spatially imprecise due to the inverse problem, it is difficult to speculate which structures contribute to the delta/theta SPE. It might be an interesting pathway for future studies to examine EEG source estimations or to add neuroimaging to gather insights into the functional connectivity of the associative self-network. This might help to understand the distinct contributions of faster and slower oscillations during self-prioritization. Our findings also bridge a gap between cognitive SPE literature and application studies in a sense that future studies might investigate frequency-specific brain stimulation of the SPE (e.g., transcranial alternating current stimulation, tACS; see Bao et al., 2021, for a current meta-analysis of brain stimulation of the SPE). Whether the oscillatory markers for the SPE in the matching task reveal to be domain specific, or whether they extend to personally relevant objects, persons, memories, etc., is a further fertile research avenue.

To conclude, our study presents spectral signatures of the self-prioritization effect in an associative matching task in the beta- and delta-/theta-frequency range. In particular, self-associated shapes were processed with increased beta and delta/theta power, compared to stranger-associated shapes. Drift-diffusion modeling suggests that evidence accumulation was associated with the SPE in beta power, whereas faster decision-making was associated with the SPE in delta/theta power. In particular, decreased beta suppression might indicate a more efficient sensorimotor integration of self-associated features into the self-network, whereas increased delta/theta power might index the facilitated retrieval of self-associated context features. These findings bring light to the spectral organization of the associative self-network in the human brain. Self-relevance might function as an associative glue for the binding and retrieval of elements in a network of importance.

AUTHOR CONTRIBUTIONS

Céline Chantal Haciahmet: Conceptualization; data curation; formal analysis; investigation; methodology; project administration; software; validation; visualization; writing – original draft; writing – review and editing. **Marius Golubickis:** Conceptualization; data curation; formal analysis; investigation; methodology; software; validation; visualization; writing – original draft; writing – review and editing. **Sarah Schäfer:** Conceptualization; funding acquisition; methodology; resources; validation; writing – review and editing. **Christian Frings:** Resources; supervision; writing – review and editing. **Bernhard Pastötter:** Conceptualization; data curation; formal analysis; methodology; project administration; resources; software; supervision; validation; writing – original draft; writing – review and editing.

ACKNOWLEDGMENTS

The authors thank Mr. Thorsten Brinkman and Mr. Joachim Paulus for their assistance with data collection

and programming. Open Access funding enabled and organized by Projekt DEAL.

FUNDING INFORMATION

The research reported in this article was supported by a Grant from the Deutsche Forschungsgemeinschaft (SCHA 2253/1–1).

CONFLICT OF INTEREST STATEMENT

The authors declare no conflict of interest regarding financial or other aspects of the publication of this study.

DATA AVAILABILITY STATEMENT

The data sets generated or analyzed during the current study are available in the Open Science Framework (OSF) repository: https://osf.io/2juxk/?view_only=b4e01124337a4801b4beb99dbe803b8d. Code for the hierarchical drift-diffusion modeling (HDDM) can be downloaded as an open-source Python toolbox from https://hddm.readthedocs.io/en/latest/.

ORCID

Céline C. Haciahmet https://orcid.org/0000-0001-5062-2551
Marius Golubickis https://orcid.org/0000-0001-6128-0331
Sarah Schäfer https://orcid.org/0000-0002-2569-0883
Christian Frings https://orcid.org/0000-0002-3852-7380
Bernhard Pastötter https://orcid.org/0000-0001-7364-4702

REFERENCES

Alexopoulos, T., Muller, D., Ric, F., & Marendaz, C. (2012). I, me, mine: Automatic attentional capture by self-related stimuli. *European Journal of Social Psychology*, *42*(6), 770–779. https://doi.org/10.1002/ejsp.1882

Alzueta, E., Melcón, M., Jensen, O., & Capilla, A. (2020). The 'Narcissus Effect': Top-down alpha-beta band modulation of face-related brain areas during self-face processing. *NeuroImage*, *213*, 116754. https://doi.org/10.1016/j.neuroimage.2020.116754

Axmacher, N., Mormann, F., Fernández, G., Elger, C. E., & Fell, J. (2006). Memory formation by neuronal synchronization. *Brain Research Reviews*, *52*(1), 170–182. https://doi.org/10.1016/j.brainresrev.2006.01.007

Başar, E., Başar-Eroğlu, C., Karakaş, S., & Schürmann, M. (2000). Brain oscillations in perception and memory. *International Journal of Psychophysiology*, *35*(2–3), 95–124. https://doi.org/10.1016/S0167-8760(99)00047-1

Battaglia, F. P., Benchenane, K., Sirota, A., Pennartz, C. M. A., & Wiener, S. I. (2011). The hippocampus: Hub of brain network communication for memory. *Trends in Cognitive Sciences*, *15*(7), 310–318. https://doi.org/10.1016/j.tics.2011.05.008

Beste, C., Münchau, A., & Frings, C. (2023). Towards a systematization of brain oscillatory activity in actions. *Communications Biology*, *6*(1), 137. https://doi.org/10.1038/s42003-023-04531-9

Bridwell, D. A., Cavanagh, J. F., Collins, A. G. E., Nunez, M. D., Srinivasan, R., Stober, S., & Calhoun, V. D. (2018). Moving beyond ERP components: A selective review of approaches to integrate EEG and behavior. *Frontiers in Human Neuroscience*, *12*, 106. https://doi.org/10.3389/fnhum.2018.00106

Cavanagh, J. F., Wiecki, T. V., Cohen, M. X., Figueroa, C. M., Samanta, J., Sherman, S. J., & Frank, M. J. (2011). Subthalamic nucleus stimulation reverses mediofrontal influence over decision threshold. *Nature Neuroscience*, *14*(11), 1462–1467. https://doi.org/10.1038/nn.2925

Cousineau, D., & O'Brien, F. (2014). Error bars in within-subject designs: A comment on Baguley (2012). *Behavior Research Methods*, *46*(4), 1149–1151. https://doi.org/10.3758/s13428-013-0441-z

Dastjerdi, M., Foster, B. L., Nasrullah, S., Rauschecker, A. M., Dougherty, R. F., Townsend, J. D., Chang, C., Greicius, M. D., Menon, V., Kennedy, D. P., & Parvizi, J. (2011). Differential electrophysiological response during rest, self-referential, and non-self-referential tasks in human posteromedial cortex. *Proceedings of the National Academy of Sciences of the United States of America*, *108*(7), 3023–3028. https://doi.org/10.1073/pnas.1017098108

Eichenlaub, J.-B., Ruby, P., & Morlet, D. (2012). What is the specificity of the response to the own first-name when presented as a novel in a passive oddball paradigm? An ERP study. *Brain Research*, *1447*, 65–78. https://doi.org/10.1016/j.brainres.2012.01.072

Erla, S., Faes, L., Nollo, G., Arfeller, C., Braun, C., & Papadelis, C. (2012). Multivariate EEG spectral analysis evidences the functional link between motor and visual cortex during integrative sensorimotor tasks. *Biomedical Signal Processing and Control*, *7*(3), 221–227. https://doi.org/10.1016/j.bspc.2011.08.002

Falbén, J. K., Golubickis, M., Wischerath, D., Tsamadi, D., Persson, L. M., Caughey, S., Svensson, S. L., & Macrae, C. N. (2020). It's not always about me: The effects of prior beliefs and stimulus prevalence on self-other prioritisation. *Quarterly Journal of Experimental Psychology*, *73*(9), 1466–1480. https://doi.org/10.1177/1747021820913016

Faul, F., Erdfelder, E., Lang, A.-G., & Buchner, A. (2007). G*power 3: A flexible statistical power analysis program for the social, behavioral, and biomedical sciences. *Behavior Research Methods*, *39*(2), 175–191. https://doi.org/10.3758/bf03193146

Forstmann, B. U., Ratcliff, R., & Wagenmakers, E.-J. (2016). Sequential sampling models in cognitive neuroscience: Advantages, applications, and extensions. *Annual Review of Psychology*, *67*, 641–666. https://doi.org/10.1146/annurev-psych-122414-033645

Forstmann, B. U., & Wagenmakers, E.-J. (2015). Model-based cognitive neuroscience: A conceptual introduction. In B. U. Forstmann & E.-J. Wagenmakers (Eds.), *An introduction to model-based cognitive neuroscience* (pp. 139–156). Springer. https://doi.org/10.1007/978-1-4939-2236-9_7

Fries, P. (2005). A mechanism for cognitive dynamics: Neuronal communication through neuronal coherence. *Trends in Cognitive Sciences*, *9*(10), 474–480. https://doi.org/10.1016/j.tics.2005.08.011

Frings, C., Hommel, B., Koch, I., Rothermund, K., Dignath, D., Giesen, C., Kiesel, A., Kunde, W., Mayr, S., Moeller, B., Möller, M., Pfister, R., & Philipp, A. (2020). Binding and retrieval in action control (BRAC). *Trends in Cognitive Sciences*, *24*(5), 375–387. https://doi.org/10.1016/j.tics.2020.02.004

Frings, C., & Wentura, D. (2014). Self-priorization processes in action and perception. *Journal of Experimental Psychology: Human Perception and Performance*, *40*(5), 1737–1740. https://doi.org/10.1037/a0037376

Golubickis, M., Falbén, J. K., Ho, N. S. P., Sui, J., Cunningham, W. A., & Neil Macrae, C. (2020). Parts of me: Identity-relevance moderates self-prioritization. *Consciousness and Cognition*, *77*, 102848. https://doi.org/10.1016/j.concog.2019.102848

Golubickis, M., Falben, J. K., Sahraie, A., Visokomogilski, A., Cunningham, W. A., Sui, J., & Macrae, C. N. (2017). Self-prioritization and perceptual matching: The effects of temporal construal. *Memory & Cognition*, *45*(7), 1223–1239. https://doi.org/10.3758/s13421-017-0722-3

Golubickis, M., & Macrae, C. N. (2021a). Judging me and you: Task design modulates self-prioritization. *Acta Psychologica*, *218*, 103350. https://doi.org/10.1016/j.actpsy.2021.103350

Golubickis, M., & Macrae, C. N. (2021b). That's me in the spotlight: Self-relevance modulates attentional breadth. *Psychonomic Bulletin & Review*, *28*(6), 1915–1922. https://doi.org/10.3758/s13423-021-01964-3

Gongora, M., Bittencourt, J., Teixeira, S., Basile, L. F., Pompeu, F., Droguett, E. L., Arias-Carrion, O., Budde, H., Cagy, M., Velasques, B., Nardi, A. E., & Ribeiro, P. (2016). Low-frequency rTMS over the parieto-frontal network during a sensorimotor task: The role of absolute beta power in the sensorimotor integration. *Neuroscience Letters*, *611*, 1–5. https://doi.org/10.1016/j.neulet.2015.11.025

Gray, H. M., Ambady, N., Lowenthal, W. T., & Deldin, P. (2004). P300 as an index of attention to self-relevant stimuli. *Journal of Experimental Social Psychology*, *40*(2), 216–224. https://doi.org/10.1016/S0022-1031(03)00092-1

He, Q., Sun, Q., Shi, Z., Zhang, X., & Hu, F. (2018). Effect of social distance on outcome evaluation in self-other decision-making: Evidence from event-related potentials. *Neuroreport*, *29*(17), 1499–1503. https://doi.org/10.1097/WNR.0000000000001141

Herweg, N. A., Solomon, E. A., & Kahana, M. J. (2020). Theta oscillations in human memory. *Trends in Cognitive Sciences*, *24*(3), 208–227. https://doi.org/10.1016/j.tics.2019.12.006

Herz, D. M., Zavala, B. A., Bogacz, R., & Brown, P. (2016). Neural correlates of decision thresholds in the human subthalamic nucleus. *Current Biology*, *26*(7), 916–920. https://doi.org/10.1016/j.cub.2016.01.051

Hoijtink, H., Mulder, J., van Lissa, C., & Gu, X. (2019). A tutorial on testing hypotheses using the Bayes factor. *Psychological Methods*, *24*(5), 539–556. https://doi.org/10.1037/met0000201

Hommel, B. (2019). Theory of event coding (TEC) V2.0: Representing and controlling perception and action. *Attention, Perception, & Psychophysics*, *81*(7), 2139–2154. https://doi.org/10.3758/s13414-019-01779-4

Hosaka, R., Nakajima, T., Aihara, K., Yamaguchi, Y., & Mushiake, H. (2016). The suppression of beta oscillations in the primate supplementary motor complex reflects a volatile state during the updating of action sequences. *Cerebral Cortex*, *26*(8), 3442–3452. https://doi.org/10.1093/cercor/bhv163

Hu, C., Di, X., Eickhoff, S. B., Zhang, M., Peng, K., Guo, H., & Sui, J. (2016). Distinct and common aspects of physical and psychological self-representation in the brain: A meta-analysis of self-bias in facial and self-referential judgements. *Neuroscience and Biobehavioral Reviews*, *61*, 197–207. https://doi.org/10.1016/j.neubiorev.2015.12.003

Imafuku, M., Hakuno, Y., Uchida-Ota, M., Yamamoto, J.-I., & Minagawa, Y. (2014). "Mom called me!" behavioral and prefrontal responses of infants to self-names spoken by their mothers. *NeuroImage*, *103*, 476–484. https://doi.org/10.1016/j.neuroimage.2014.08.034

Jacobs, J., Hwang, G., Curran, T., & Kahana, M. J. (2006). EEG oscillations and recognition memory: Theta correlates of memory retrieval and decision making. *NeuroImage*, *32*(2), 978–987. https://doi.org/10.1016/j.neuroimage.2006.02.018

James, W. (1890). *The principles of psychology* (Vol. *1*). Henry Holt and Company. https://mindsplain.com/wp-content/uploads/2020/08/the-principles-of-psychology-i-by-william-james_.pdf

JASP Team. (2022). *JASP* (Version 0.16.3) [Computer software].

Karakaş, S. (2020). A review of theta oscillation and its functional correlates. *International Journal of Psychophysiology*, *157*, 82–99. https://doi.org/10.1016/j.ijpsycho.2020.04.008

Keyes, H., Brady, N., Reilly, R. B., & Foxe, J. J. (2010). My face or yours? Event-related potential correlates of self-face processing. *Brain and Cognition*, *72*(2), 244–254. https://doi.org/10.1016/j.bandc.2009.09.006

Keyes, H., & Dlugokencka, A. (2014). Do I have my attention? Speed of processing advantages for the self-face are not driven by automatic attention capture. *PLoS One*, *9*(10), e110792. https://doi.org/10.1371/journal.pone.0110792

Kiesel, A., Fournier, L. R., Giesen, C. G., Mayr, S., & Frings, C. (2023). Core mechanisms in action control: Binding and retrieval. *Journal of Cognition*, *6*(1), 2. https://doi.org/10.5334/joc.253

Knyazev, G. G. (2013). EEG correlates of self-referential processing. *Frontiers in Human Neuroscience*, *7*, 264. https://doi.org/10.3389/fnhum.2013.00264

Lee, D. G., Daunizeau, J., & Pezzulo, G. (2023). Evidence or confidence: What is really monitored during a decision? *Psychonomic Bulletin & Review*. https://doi.org/10.3758/s13423-023-02255-9

Lenggenhager, B., Halje, P., & Blanke, O. (2011). Alpha band oscillations correlate with illusory self-location induced by virtual reality. *The European Journal of Neuroscience*, *33*(10), 1935–1943. https://doi.org/10.1111/j.1460-9568.2011.07647.x

Liebrand, M., Kristek, J., Tzvi, E., & Krämer, U. M. (2018). Ready for change: Oscillatory mechanisms of proactive motor control. *PLoS One*, *13*(5), e0196855. https://doi.org/10.1371/journal.pone.0196855

Ma, Y., & Han, S. (2010). Why we respond faster to the self than to others? An implicit positive association theory of self-advantage during implicit face recognition. *Journal of Experimental Psychology. Human Perception and Performance*, *36*(3), 619–633. https://doi.org/10.1037/a0015797

Macrae, C. N., Visokomogilski, A., Golubickis, M., Cunningham, W. A., & Sahraie, A. (2017). Self-relevance prioritizes access to visual awareness. *Journal of Experimental Psychology. Human Perception and Performance*, *43*(3), 438–443. https://doi.org/10.1037/xhp0000361

Memelink, J., & Hommel, B. (2013). Intentional weighting: A basic principle in cognitive control. *Psychological Research*, *77*(3), 249–259. https://doi.org/10.1007/s00426-012-0435-y

Miyakoshi, M., Kanayama, N., Iidaka, T., & Ohira, H. (2010). EEG evidence of face-specific visual self-representation. *NeuroImage*, *50*(4), 1666–1675. https://doi.org/10.1016/j.neuroimage.2010.01.030

Moran, J. M., Heatherton, T. F., & Kelley, W. M. (2009). Modulation of cortical midline structures by implicit and explicit self-relevance evaluation. *Social Neuroscience*, *4*(3), 197–211. https://doi.org/10.1080/17470910802250519

Moray, N. (1959). Attention in dichotic listening: Affective cues and the influence of instructions. *Quarterly Journal of Experimental Psychology*, *11*(1), 56–60. https://doi.org/10.1080/17470215908416289

Morel, N., Villain, N., Rauchs, G., Gaubert, M., Piolino, P., Landeau, B., Mézenge, F., Desgranges, B., Eustache, F., & Chételat, G. (2014). Brain activity and functional coupling changes associated with self-reference effect during both encoding and retrieval. *PLoS One*, *9*(3), e90488. https://doi.org/10.1371/journal.pone.0090488

Mu, Y., & Han, S. (2010). Neural oscillations involved in self-referential processing. *NeuroImage*, *53*(2), 757–768. https://doi.org/10.1016/j.neuroimage.2010.07.008

Mu, Y., & Han, S. (2013). Neural oscillations dissociate between self-related attentional orientation versus evaluation. *NeuroImage*, *67*, 247–256. https://doi.org/10.1016/j.neuroimage.2012.11.016

Murray, R. J., Debbané, M., Fox, P. T., Bzdok, D., & Eickhoff, S. B. (2015). Functional connectivity mapping of regions associated with self- and other-processing. *Human Brain Mapping*, *36*(4), 1304–1324. https://doi.org/10.1002/hbm.22703

Nayak, S., Kuo, C., & Tsai, A. C.-H. (2019). Mid-frontal theta modulates response inhibition and decision making processes in emotional contexts. *Brain Sciences*, *9*(10), 271. https://doi.org/10.3390/brainsci9100271

Nijhof, A. D., von Trott Zu Solz, J., Catmur, C., & Bird, G. (2022). Equivalent own name bias in autism: An EEG study of the attentional blink. *Cognitive, Affective, & Behavioral Neuroscience*, *22*(3), 625–639. https://doi.org/10.3758/s13415-021-00967-w

Pastötter, B., & Bäuml, K.-H. T. (2014). Distinct slow and fast cortical theta dynamics in episodic memory retrieval. *NeuroImage*, *94*, 155–161. https://doi.org/10.1016/j.neuroimage.2014.03.002

Pastötter, B., Berchtold, F., & Bäuml, K.-H. T. (2012). Oscillatory correlates of controlled speed-accuracy tradeoff in a response-conflict task. *Human Brain Mapping*, *33*(8), 1834–1849. https://doi.org/10.1002/hbm.21322

Pastötter, B., Moeller, B., & Frings, C. (2021). Watching the brain as it (un)binds: Beta synchronization relates to distractor-response binding. *Journal of Cognitive Neuroscience*, *33*(8), 1581–1594. https://doi.org/10.1162/jocn_a_01730

Pfurtscheller, G., & Aranibar, A. (1977). Event-related cortical desynchronization detected by power measurements of scalp EEG. *Electroencephalography and Clinical Neurophysiology*, *42*(6), 817–826. https://doi.org/10.1016/0013-4694(77)90235-8

Qin, P., Wang, M., & Northoff, G. (2020). Linking bodily, environmental and mental states in the self-a three-level model based on a meta-analysis. *Neuroscience and Biobehavioral Reviews*, *115*, 77–95. https://doi.org/10.1016/j.neubiorev.2020.05.004

Ratcliff, R., Smith, P. L., Brown, S. D., & McKoon, G. (2016). Diffusion decision model: Current issues and history. *Trends in Cognitive Sciences*, *20*(4), 260–281. https://doi.org/10.1016/j.tics.2016.01.007

Schäfer, S., Wentura, D., & Frings, C. (2015). Self-prioritization beyond perception. *Experimental Psychology*, *62*(6), 415–425. https://doi.org/10.1027/1618-3169/a000307

Schäfer, S., Wentura, D., & Frings, C. (2020). Creating a network of importance: The particular effects of self-relevance on stimulus processing. *Attention, Perception & Psychophysics*, *82*(7), 3750–3766. https://doi.org/10.3758/s13414-020-02070-7

Siegel, M., Engel, A. K., & Donner, T. H. (2011). Cortical network dynamics of perceptual decision-making in the human brain. *Frontiers in Human Neuroscience*, *5*, 21. https://doi.org/10.3389/fnhum.2011.00021

Spiegelhalter, D. J., Best, N. G., & Carlin, B. P. (1998). *Bayesian deviance, the effective number of parameters, and the comparison of arbitrarily complex models*. Research Report, 98–009.

Sui, J., & Han, S. (2007). Self-construal priming modulates neural substrates of self-awareness. *Psychological Science*, *18*(10), 861–866. https://doi.org/10.1111/j.1467-9280.2007.01992.x

Sui, J., He, X., Golubickis, M., Svensson, S. L., & Neil Macrae, C. (2023). Electrophysiological correlates of self-prioritization. *Consciousness and Cognition*, *108*, 103475. https://doi.org/10.1016/j.concog.2023.103475

Sui, J., He, X., & Humphreys, G. W. (2012). Perceptual effects of social salience: Evidence from self-prioritization effects on perceptual matching. *Journal of Experimental Psychology. Human Perception and Performance*, *38*(5), 1105–1117. https://doi.org/10.1037/a0029792

Sui, J., & Humphreys, G. W. (2015). The integrative self: How self-reference integrates perception and memory. *Trends in Cognitive Sciences*, *19*(12), 719–728. https://doi.org/10.1016/j.tics.2015.08.015

Sui, J., & Rotshtein, P. (2019). Self-prioritization and the attentional systems. *Current Opinion in Psychology*, *29*, 148–152. https://doi.org/10.1016/j.copsyc.2019.02.010

Sui, J., Zhu, Y., & Han, S. (2006). Self-face recognition in attended and unattended conditions: An event-related brain potential study. *Neuroreport*, *17*(4), 423–427. https://doi.org/10.1097/01.wnr.0000203357.65190.61

Svensson, S. L., Golubickis, M., Maclean, H., Falbén, J. K., Persson, L. M., Tsamadi, D., Caughey, S., Sahraie, A., & Macrae, C. N. (2022). More or less of me and you: Self-relevance augments the effects of item probability on stimulus prioritization. *Psychological Research*, *86*(4), 1145–1164. https://doi.org/10.1007/s00426-021-01562-x

Tacikowski, P., Cygan, H. B., & Nowicka, A. (2014). Neural correlates of own and close-other's name recognition: ERP evidence. *Frontiers in Human Neuroscience*, *8*, 194. https://doi.org/10.3389/fnhum.2014.00194

Ulrich, R., Schröter, H., Leuthold, H., & Birngruber, T. (2015). Automatic and controlled stimulus processing in conflict tasks: Superimposed diffusion processes and delta functions. *Cognitive Psychology*, *78*, 148–174. https://doi.org/10.1016/j.cogpsych.2015.02.005

Vandekerckhove, J., Tuerlinckx, F., & Lee, M. D. (2011). Hierarchical diffusion models for two-choice response times. *Psychological Methods*, *16*(1), 44–62. https://doi.org/10.1037/a0021765

Verguts, T., & Notebaert, W. (2009). Adaptation by binding: A learning account of cognitive control. *Trends in Cognitive Sciences*, *13*(6), 252–257. https://doi.org/10.1016/j.tics.2009.02.007

Voss, A., Nagler, M., & Lerche, V. (2013). Diffusion models in experimental psychology: A practical introduction. *Experimental Psychology*, *60*(6), 385–402. https://doi.org/10.1027/1618-3169/a000218

White, C. N., & Poldrack, R. A. (2014). Decomposing bias in different types of simple decisions. *Journal of Experimental Psychology.*

Learning, Memory, and Cognition, *40*(2), 385–398. https://doi.org/10.1037/a0034851

Wiecki, T. V., Sofer, I., & Frank, M. J. (2013). HDDM: Hierarchical Bayesian estimation of the drift-diffusion model in python. *Frontiers in Neuroinformatics*, *7*, 14. https://doi.org/10.3389/fninf.2013.00014

Woźniak, M., & Knoblich, G. (2019). Self-prioritization of fully unfamiliar stimuli. *Quarterly Journal of Experimental Psychology (2006)*, *72*(8), 2110–2120. https://doi.org/10.1177/1747021819832981

Woźniak, M., Kourtis, D., & Knoblich, G. (2018). Prioritization of arbitrary faces associated to self: An EEG study. *PLoS One*, *13*(1), e0190679. https://doi.org/10.1371/journal.pone.0190679

Yankouskaya, A., Humphreys, G., Stolte, M., Stokes, M., Moradi, Z., & Sui, J. (2017). An anterior-posterior axis within the ventromedial prefrontal cortex separates self and reward. *Social Cognitive and Affective Neuroscience*, *12*(12), 1859–1868. https://doi.org/10.1093/scan/nsx112

Yankouskaya, A., & Sui, J. (2021). Self-positivity or self-negativity as a function of the medial prefrontal cortex. *Brain Sciences*, *11*(2), 264. https://doi.org/10.3390/brainsci11020264

Yankouskaya, A., & Sui, J. (2022). Self-prioritization is supported by interactions between large-scale brain networks. *The European Journal of Neuroscience*, *55*(5), 1244–1261. https://doi.org/10.1111/ejn.15612

Yau, Y., Hinault, T., Taylor, M., Cisek, P., Fellows, L. K., & Dagher, A. (2021). Evidence and urgency related EEG signals during dynamic decision-making in humans. *The Journal of Neuroscience*, *41*(26), 5711–5722. https://doi.org/10.1523/JNEUROSCI.2551-20.2021

Yin, S., Bi, T., Chen, A., & Egner, T. (2021). Ventromedial prefrontal cortex drives the prioritization of self-associated stimuli in working memory. *The Journal of Neuroscience*, *41*(9), 2012–2023. https://doi.org/10.1523/JNEUROSCI.1783-20.2020

Zhou, A., Shi, Z., Zhang, P., Liu, P., Han, W., Wu, H., Li, Q., Zuo, Q., & Xia, R. (2010). An ERP study on the effect of self-relevant possessive pronoun. *Neuroscience Letters*, *480*(2), 162–166. https://doi.org/10.1016/j.neulet.2010.06.033

Bao, Z., Howidi, B., Burhan, A. M., & Frewen, P. (2021). Self-referential processing effects of non-invasive brain stimulation: A systematic review. *Frontiers in Neuroscience*, *15*, 671020. https://doi.org/10.3389/fnins.2021.671020.

SUPPORTING INFORMATION

Additional supporting information can be found online in the Supporting Information section at the end of this article.

Appendix S1. Reports event-related potential (ERP) results for the matching task and methods and results for the flanking shape classification task.

How to cite this article: Haciahmet, C. C., Golubickis, M., Schäfer, S., Frings, C., & Pastötter, B. (2023). The oscillatory fingerprints of self-prioritization: Novel markers in spectral EEG for self-relevant processing. *Psychophysiology*, *60*, e14396. https://doi.org/10.1111/psyp.14396